

Dalton Transactions

Accepted Manuscript



This is an *Accepted Manuscript*, which has been through the Royal Society of Chemistry peer review process and has been accepted for publication.

Accepted Manuscripts are published online shortly after acceptance, before technical editing, formatting and proof reading. Using this free service, authors can make their results available to the community, in citable form, before we publish the edited article. We will replace this *Accepted Manuscript* with the edited and formatted *Advance Article* as soon as it is available.

You can find more information about *Accepted Manuscripts* in the [Information for Authors](#).

Please note that technical editing may introduce minor changes to the text and/or graphics, which may alter content. The journal's standard [Terms & Conditions](#) and the [Ethical guidelines](#) still apply. In no event shall the Royal Society of Chemistry be held responsible for any errors or omissions in this *Accepted Manuscript* or any consequences arising from the use of any information it contains.

Correlation of crystal structure and microwave dielectric properties of $\text{Nd}_{1.02}(\text{Nb}_{1-x}\text{Ta}_x)_{0.988}\text{O}_4$ ceramic

Ping Zhang*, Yonggui Zhao, Jian Liu, Zhenkun Song, Mi Xiao, Xiuyu Wang

School of Electronic and Information Engineering, Tianjin University, Tianjin 300072, China

Abstract

The phase structure of $\text{Nd}_{1.02}(\text{Nb}_{1-x}\text{Ta}_x)_{0.988}\text{O}_4$ ceramics were analyzed via multiphase structure refinement. The X-ray diffraction patterns of $\text{Nd}_{1.02}(\text{Nb}_{1-x}\text{Ta}_x)_{0.988}\text{O}_4$ showed that the monoclinic fergusonite structure of NdNbO_4 and the second phase $\text{NdTa}_7\text{O}_{19}$ were obtained. The oxygen octahedron distortion was investigated according to the supercell of the NdNbO_4 ceramic. The correlation between packing fractions, bond valence and microwave dielectric properties were discussed. For the main phase NdNbO_4 , with the polarizabilities increasing, the ϵ increased. The $Q \times f$ value was mainly attributed to the packing fraction. With the increase of bond valence of B-site and the oxygen octahedron distortion, the τ_f value decreased. The substitution of Ta^{5+} for Nb^{5+} effectively influenced the microstructure and the microwave dielectric properties of NdNbO_4 ceramics. An optimal microwave dielectric properties can be obtained for $\text{Nd}_{1.02}(\text{Nb}_{0.94}\text{Ta}_{0.06})_{0.988}\text{O}_4$ ceramics at $x=0.06$.

Keywords: Microstructure; Substitution; Packing fraction; Band valence; Oxygen octahedron distortion

1. Introduction

The microwave dielectric ceramic is used in the microwave band and is very effective for making smaller devices and improving the packaging density of microwave integrated circuits. For this reason, it is widely used for filters for mobile communication apparatuses (for base station and terminals) including cell phones, microwave transmitting circuit for receiving satellite broadcasting, GPS antenna, Bluetooth, and

*Corresponding author. Tel. : +86 13702194791

Email address: zptaitju@163.com (P. Zhang)

recently for ITS (Intelligent Transportation System) [1, 2].

The monoclinic fergusonite structure material NdNbO_4 with $Q \times f$ of 33,000 GHz, ϵ_r of 19.6, and τ_f of $-24 \text{ ppm}/^\circ\text{C}$ was firstly reported by *Kim.et al* [3]. In our previous study, we have studied the microwave dielectric properties of NdNbO_4 doping with CaF_2 . NdNbO_4 ceramics with 2.0 wt.% CaF_2 sintered at 1225°C for 4h possesses excellent microwave dielectric properties, $Q \times f \sim 75,000 \text{ GHz}$ and $\tau_f \sim -19 \text{ ppm}/^\circ\text{C}$ [4]. And we have also presented the effect of CaTiO_3 addition on the microwave dielectric properties of NdNbO_4 ceramic. The τ_f of $\text{NdNbO}_4\text{-CaTiO}_3$ system has a trend of shifting toward zero in the whole range. A optical $Q \times f$ of 70,000 GHz was obtained from NdNbO_4 ceramic doped with 0.6 wt.% CaTiO_3 sintered at 1275°C for 4 h [5]. Then we have studied the Mn^{2+} substitution on the microwave dielectric properties of $(\text{Nd}_{1-x}\text{Mn}_{1.5x})_{1.02}\text{Nb}_{0.988}\text{O}_4$, with $x=0.03$ Mn^{2+} addition the optimal $Q \times f$ values of NdNbO_4 can be obtained [6]. However, few works about the correlation between microstructure and microwave dielectric properties of the NdNbO_4 was not discussed.

In the following study, the correlation between microstructure and microwave dielectric properties of $\text{Nd}_{1.02}(\text{Nb}_{1-x}\text{Ta}_x)_{0.988}\text{O}_4$, packing fractions, bond valences and oxygen octahedron distortion were systematically investigated. In addition, an available method based on the Rietveld refinement of X-ray techniques was also used to analyze the structures of crystalline phases.

2. Experimental procedure

$\text{Nd}_{1.02}(\text{Nb}_{1-x}\text{Ta}_x)_{0.988}\text{O}_4$ microwave dielectric ceramics were prepared by a conventional solid-state reaction from oxide powders (Nd_2O_3 , Nb_2O_5 and Ta_2O_5) method. The purity levels are 99.9%. The raw materials were mixed according to the formula of $\text{Nd}_{1.02}(\text{Nb}_{1-x}\text{Ta}_x)_{0.988}\text{O}_4$ ($x=0.0, 0.02, 0.04, 0.06, 0.08, 0.1$). The mixed powders were milled 6 h with distilled water in a nylon container with ZrO_2 balls. All the

slurries were dried and pre-sintered at 1000 °C for 4 h. The pre-sintered powders were re-milled 6 h. After drying and sieving, the powders were pressed into pellets with 10 mm diameter and 5 mm thickness. Then these pellets were sintered at temperatures of 1275°C for 4 h.

The crystalline phases of the sintered samples were identified by X-ray diffraction (XRD, Rigaku D/max 2550 PC, Tokyo, Japan) with Cu K α radiation generated at 40 kV and 40 mA. The microwave dielectric properties were measured in the frequency range of 8-12 GHz using a HP8720ES network analyzer [7]. The temperature coefficients of resonant frequency (τ_f) were measured in the temperature range from 25 °C to 85 °C. The τ_f (ppm/°C) was calculated by noting the change in resonant frequency (Δf)

$$\tau_f = \frac{f_2 - f_1}{f_1(T_2 - T_1)} \quad (1)$$

where f_1 is resonant frequency at T_1 and f_2 is the resonant frequency at T_2 .

3. Results and discussion

3.1 Multiphase refinement

The X-ray diffraction patterns of Nd_{1.02}(Nb_{1-x}Ta_x)_{0.988}O₄ (x=0.0, 0.02, 0.04, 0.06, 0.08, 0.1) ceramics are given in Fig. 1. To reduce noise, all data had been smoothed by Adaptive smoothing method and had deducted background using Powder X [8]. All parameters of interest including background, zero-point, scale factors for all phases, half-width, asymmetry parameters, unit-cell parameters, atomic positional coordinates, temperature factors were refined step-by-step for avoiding correlations. A pure single-phase NdNbO₄ (ICDD #32-0680) without any secondary phase was observed in the range of x=0-0.06 from the diffraction patterns and it was belong to the monoclinic fergusonite structure with the space group I2/a (no. 15). The lattice parameters from Rietveld refinement were calculated as a=5.146 Å, b=11.290 Å, and

$c=5.457 \text{ \AA}$. With the substitution content increased, the $\text{NdTa}_3\text{O}_{19}$ peaks (indexed as $\text{NdTa}_3\text{O}_{19}$, ICDD #37-1319) can be detected when $x \geq 0.08$. The formation of $\text{NdTa}_3\text{O}_{19}$ could attribute to the reaction of the Nd^{3+} with the unsubstituted Ta^{5+} . The part of refinement results shown in the Table. 1. As Ta_2O_5 content increase, there was a reduction of the a-axis and b-axis of NdNbO_4 , leading to the decrease in the unit cell volume of it. According to the PDF (ICDD #33-0941), the lattice parameters of pure NdTaO_4 are $a=5.514 \text{ \AA}$, $b=11.263 \text{ \AA}$, $c=5.115 \text{ \AA}$, and $V_{\text{unit}}=315.3 \text{ \AA}^3$, and it has the same monoclinic fergusonite structure and the space group $I2/a$ (no. 15) with the pure NdNbO_4 . The substitution of Ta^{5+} ((ionic radius, abbr. $r=0.64 \text{ \AA}$, coordination numbers, abbr. CN = 8)) ion was same with the Nb^{5+} ((ionic radius, abbr. $r=0.64 \text{ \AA}$, coordination numbers, abbr. CN = 8)) ion. Therefore, the substitution of Nb^{5+} ion by Ta^{5+} could decrease the volume of the unit cell.

3.2 structure analysis

NdNbO_4 performs the monoclinic fergusonite structure. In addition, it belongs to the space group $I2/a$ (no. 15) and contains four NdNbO_4 molecules per primitive cell. Fig.2 shows a schematic representation of NdNbO_4 supercell ($1 \times 1 \times 1$). In the supercell, we can see that the NdNbO_4 consists of oxygen octahedral, and the Nb ion is the center of the oxygen octahedral in the direction of the a- axis.

With the substitution of the Ta^{5+} , the atomic interactions of NdNbO_4 in $\text{Nd}_{1.02}(\text{Nb}_{1-x}\text{Ta}_x)_{0.988}\text{O}_4$ ceramics should be changed, which could be resulted in the structure changes, such as distortion of oxygen octahedral and bond valence of B-site. The distortion of oxygen octahedral and bond valence of B-site calculated from Rietveld Refinement shown in Table. 2.

In this work, the distortion of an octahedron was defined as [9]:

$$\Delta_{\text{octahedron}} = \frac{B - \text{Odistance}_{\text{largest}} - B - \text{Odistance}_{\text{smallest}}}{B - \text{Odistance}_{\text{average}}} \quad (1)$$

The bond valence of atom i , V_{ij} was defined as the sum of all of the valences from a given atom i , and that was calculated in the Eq. (2) and (3) [10].

$$V_{ij} = \sum v_{ij} \quad (2)$$

$$v_{ij} = \exp\left(\frac{R_{ij} - d_{ij}}{b'}\right) \quad (3)$$

where R_{ij} is the bond valence parameter, d_{ij} is the length of a bond between atom i and j , and b' is commonly taken to be a universal constant equal to 0.37. With the increase of Ta^{5+} substitution, the distortion of oxygen octahedron and the bond valence of B-site increased.

3.3. Microwave dielectric properties analysis

At microwave frequencies, the dielectric constant is not only dependent on the dielectric polarizabilities, but also on the structural characteristics such as the distortion, tilting, and/or rattling spaces of oxygen octahedral in unit cell [11-13]. The observed dielectric polarizability ($\alpha_{obs.}$) was calculated to evaluate the structural dependence of the dielectric constant with comparing of the theoretical dielectric polarizability ($\alpha_{theo.}$). From the Clausius-Mosotti equation, the observed ($\alpha_{obs.}$) dielectric polarizability was calculated by the Eq. (4) [11]:

$$\alpha_{obs.} = \frac{V_m(\varepsilon - 1)}{b(\varepsilon + 2)} \quad (4)$$

and from the additive rule of dielectric polarizability, the theoretical ($\alpha_{theo.}$) dielectric polarizability was calculated by the Eq. (5) [11]:

$$\alpha_{theo.}(ABO_4) = \alpha_A + \alpha_B + \alpha_O \times 4 \quad (5)$$

where $\alpha_{obs.}$ and $\alpha_{theo.}$ are the observed and the theoretical polarizability; α_A , α_B , α_O are the ionic polarizability of A-, B-site ion, and oxygen; ε is the measured dielectric constant; b is $4\pi/3$, and V_m is molar volume, respectively.

Table.3 shows the change of the theoretical and observed dielectric polarizabilities of the NdNbO_4 specimens with the value of x . With the increase of x , both the theoretical and the deviations (Δ) between theoretical and observed dielectric increased. Then has a trend of decreasing when the second phase of $\text{NdTa}_3\text{O}_{19}$ appears. From the Fig.3, we can find that the ϵ have a similar trend with the the deviations (Δ) between theoretical and observed dielectric. Those results could be attributed to the following reasons: firstly, the theoretical polarizabilities increased. Secondly, increase B-site bond valence indicated that the bonding strength between oxygen and B ion is stronger. This suggests that the B cations of the specimens rattling hardly, which the contribution of rattling effect to the polarizabilities of the specimens was decrease, and subsequently the dielectric constant decrease.

The $Q \times f$ values were believed to be affected by many factors, and it can be divided into two fields, the intrinsic loss and extrinsic loss. The intrinsic losses are mainly caused by lattice vibration modes, while the extrinsic losses are dominated by second phases, oxygen vacancies, grain boundaries, and densification or porosity [14]. In our study, when $x \leq 0.60$, there is a single pure phase, the $Q \times f$ value is mainly affected by the intrinsic losses of the ceramics. *Kim et al.* [15] reported that $Q \times f$ value was closely related to the packing fraction of the structure. With the increasing of the packing fraction, the $Q \times f$ value would increase. This change is because of with the increase of the packing fraction, the lattice vibrations decreased. Therefore, the intrinsic loss decreases and $Q \times f$ value increases. In this work, the packing fraction is dependent on the unit cell volume; the packing fractions calculated using the following formula:

$$\begin{aligned} \text{Packing fraction}(\%) &= \frac{\text{volume of the atoms in the cell}}{\text{volume of primitive unit cell}} \\ &= \frac{\text{volume of the atoms in the cell}}{\text{volume of unit cell}} \times Z \end{aligned} \quad (6)$$

where Z is the number of formula units per unit cell. As showed in the Fig.4, with decrease of the unit cell

volume, the packing fraction would increase, and the $Q \times f$ value increased. When $x \geq 0.08$, the second phase was formed from the Fig. 1. Therefore, with the increase of Ta^{5+} substitution, $Q \times f$ value decreased. Detail dates about effective ionic radius (r_A, r_B, r_C), the unit cell volume (V_{unit}), coordination number (Z) and packing fraction (P.F) of $\text{Nd}_{1.02}(\text{Nb}_{1-x}\text{Ta}_x)_{0.988}\text{O}_4$ ($x=0.0, 0.02, 0.04, 0.06, 0.08, 0.1$) ceramics are shown in the Table.4.

It is well known that the τ_f value is a function of the temperature coefficient of the dielectric constant (τ_ϵ) and the linear thermal expansion coefficient (α_L), as show in Eq.(7) [16]:

$$\tau_f = -\frac{\tau_\epsilon}{2} - \alpha_L \quad (7)$$

In general, α_L is typically constant (~ 10 ppm/ $^\circ\text{C}$) in dielectric ceramics, while τ_ϵ depends on the tilting of oxygen octahedral [15]. *Reaney et al.* [16] have reported that the structural characteristics of [BO6] oxygen octahedral has a closely relation with τ_f , and τ_f will decrease with the increasing degree of tilting on oxygen octahedral. The bond valence and bond length between the octahedral-site cation and oxygen will affect the degree of tilting on oxygen octahedral. The τ_f value decreased as the bond valence of the oxygen octahedral site increased [13].

In this paper, the decreased τ_f value was mainly attributed to the B-site bond valence and oxygen octahedral distortion. With increase the Ta content, the B-site bond valence and the oxygen octahedral distortion increased. This would be lead to decrease of τ_f .

The optimal microwave dielectric properties with $\epsilon = 21.66$, $Q \times f = 51,000$ GHz, $\tau_f = -45.7$ ppm/ $^\circ\text{C}$ were obtained for $\text{Nd}_{1.02}(\text{Nb}_{1-x}\text{Ta}_x)_{0.988}\text{O}_4$ ($x=0.06$) ceramics.

4. Conclusions

The multiphase refinement was used to analysis the crystal structure of NdNbO_4 . The distortion of

oxygen octahedral and bond valence of B-site were calculated from Rietveld refinement. The effects of Ta⁵⁺ substitution on the microstructures and microwave dielectric properties of NdNbO₄ ceramics have been discussed and the quality factor was found to decrease with presence of second phase. The cell parameters were used for the explanation of the microwave dielectric properties. The dielectric constant ϵ_r was dependent on dielectric polarizabilities. The $Q \times f$ value increased with the increase in packing fraction, because of the effective ionic radii and cell volume. The τ_f of the specimens had a close relation with the structural characteristics of [NbO₆] oxygen octahedral and decreased with increase of B-site bond valence, the oxygen octahedral distortion. An optimal microwave dielectric properties with $\epsilon_r = 21.66$, $Q \times f = 51,000$ GHz, $\tau_f = -45.7$ ppm/°C can be obtained for Nd_{1.02}(Nb_{1-x}Ta_x)_{0.988}O₄ (x=0.06) ceramics.

References

- 1 Y. B. Chen. *J. All. Comp.*, 2009,478,781-784.
- 2 D. W. Kim, D. Y. Kim and K. S. Hong, *J. Mater. Res.*, 2000, 15(6),1331-1335.
- 3 D. W. Kim, D. K. Kwon, S. H. Yoon, K. S. Hong, *J. Am. Ceram. Soc.*, 2006,89 (12), 3861-3864.
- 4 P. Zhang, T. Wang, W. S. Xia, L. X. Li, *J. Alloy. Compd.*, 2012,53,51-54.
- 5 P. Zhang, Z. K. Song, Y. Wang, Y. M. Han, H. L. Dong, L. X. Li, *J. Alloy. Compd.*, 2013,581, 741-746.
- 6 Z. K. Song, P. Zhang, Y. Wang, L. X. Li, *J. Alloy. Compd.*, 2014,583,546-549.
- 7 W. E. Courtney. *IEEE Trans Microwave Theory Tech.*, 1970,18 (8),476-485.
- 8 C. Dong, *J. Appl. Crystallogr.*, 1999, 32, 838.
- 9 F. Lichtenberg, A. Herrnberger, K. Wiedenmann, *J. Solid. State. Chem.*, 2008,36, 253-387.
- 10 P. Zhang, Z. K. Song, Y. Wang, L.X. Li, *J. Am. Ceram. Soc.*, 2014,97(3),976-981.
- 11 Q. W. Liao, L. X. Li, *Dalton. Trans.*, 2012, 41, 6963-6969.

- 12 D. Zhou , Li X. Pang, H. Wang, X. Yao, *Solid. State. Sci.*,2009,11,1894-1197.
- 13 R. D. Shannon, *J. Appl. Phys.*, 1993,73 (1),348-366.
- 14 C, L, Huang, S, S, Liu, *J. Appl. Phys.*, 2007,46,283-285.
- 15 W. S. Kim, K. H. Yoon, and E. S. Kim, *J. Am. Ceram. Soc.*, 2008,83(9),2327-2329.
- 16 I. M. Reaney, E. L. Colla, and N. Setter, *Jpn. Appl. Phys.*, 1994, 33,3984-3990

Table. 1 Crystallographic data from Rietveld refinement for $\text{Nd}_{1.02}(\text{Nb}_{1-x}\text{Ta}_x)_{0.988}\text{O}_4$ ($x=0.0, 0.02, 0.04, 0.06, 0.08, 0.1$) ceramics.

Value of x	Lattice parameters(\AA)			$V_{\text{unit}} (\text{\AA}^3)$	Reliability factors		
	a	b	c		R_p	R_{wp}	GOF
0	5.146	11.290	5.457	317.26	0.067	0.102	1.457
0.02	5.148	11.285	5.450	316.92	0.071	0.121	1.432
0.04	5.147	11.278	5.466	316.31	0.082	0.114	1.323
0.06	5.145	11.273	5.463	315.86	0.057	0.099	1.397
0.08	5.144	11.274	5.460	315.48	0.064	1.106	1.532
0.10	5.141	11.267	5.457	315.23	0.057	1.109	1.168

Table. 2 Oxygen octahedron distortion, B-site bond valence $V_{\text{B-O}}$ and τ_f of $\text{Nd}_{1.02}(\text{Nb}_{1-x}\text{Ta}_x)_{0.988}\text{O}_4$ ($x=0.0, 0.02, 0.04, 0.06, 0.08, 0.1$) specimens.

Value of x	$d_{\text{B-O}}(\text{\AA})$	$R_{\text{B-O}}(\text{\AA})$	$v_{\text{B-O}}(\text{\AA})$	$V_{\text{B-O}}(\text{\AA})$	$\Delta_{\text{octahedron}}(\%)$	$\tau_f(\text{ppm}/^\circ\text{C})$
0	1.8688	1.8881	1.0535	2.2480	29.550	-36.1
	1.8901		0.9946			
	2.4837		0.8199			
0.02	1.8678	1.8882	1.0567	2.2565	29.558	-40.7
	1.8885		0.9992			
	2.4825		0.2006			
0.04	1.8669	1.8884	1.0598	2.2599	29.565	-43.3
	1.8888		0.9989			
	2.4816		0.2012			

0.06	1.8655	1.8886	1.0644	2.2671	29.570	-45.7
	1.8872		1.0004			
	2.4798		0.2023			
0.08	1.8646	1.8888	1.0676	2.2784	29.584	-46.1
	1.8859		1.0079			
	2.4789		0.2029			
0.1	1.8663	1.8890	1.0633	2.2808	29.593	-46.4
	1.8833		1.0155			
	2.4809		0.2020			

Table. 3 Comparison of theoretical and observed polarizabilities of $\text{Nd}_{1.02}(\text{Nb}_{1-x}\text{Ta}_x)_{0.988}\text{O}_4$ ($x=0.0, 0.02, 0.04, 0.06, 0.08, 0.1$) specimens.

Value of x	$\alpha_{theo.}$	observed				$\Delta, \%$ ($\alpha_{obs}-\alpha_{theo.}$) / $\alpha_{obs} \times 100$
		ϵ	$V_{unit}(\text{\AA}^3)$	Z	α_{obs}	
0	17.0726	19.82	317.26	4	16.3317	-4.5366
0.02	17.0876	20.27	316.92	4	16.3668	-4.4040
0.04	17.1026	21.13	316.31	4	16.4298	-4.0950
0.06	17.1176	21.66	315.86	4	16.4612	-3.9876
0.08	17.1326	21.41	315.48	4	16.4159	-4.3659
0.10	17.1476	19.88	315.23	4	16.2343	-5.3621

Table. 4 Effective ionic radius (r_A , r_B , r_C), the unit cell volume(V_{unit}), coordination number (Z) and packing fraction (P.F) of $Nd_{1.02}(Nb_{1-x}Ta_x)_{0.988}O_4$ ($x=0.0, 0.02, 0.04, 0.06, 0.08, 0.1$) ceramics.

Value of x	r_A (Å)	r_B (Å)	r_C (Å)	V_{unit} (Å ³)	Z	Q×f	P.F (%)
0	1.131	0.632	1.42	317.26	4	35070	69.46
0.02	1.131	0.632	1.42	316.92	4	36640	69.53
0.04	1.131	0.632	1.42	316.31	4	40100	69.67
0.06	1.131	0.632	1.42	315.86	4	51000	69.77
0.08	1.131	0.632	1.42	315.48	4	46360	69.85
0.10	1.131	0.632	1.42	315.23	4	33200	69.91

Figure Captions

Fig.1 The X-ray diffraction patterns of $\text{Nd}_{1.02}(\text{Nb}_{1-x}\text{Ta}_x)_{0.988}\text{O}_4$ ($x=0.0, 0.02, 0.04, 0.06, 0.08, 0.1$) ceramics.

Fig.2 The crystal structure patterns of NdNbO_4 : (a) $(1 \times 1 \times 1)$ supercell of ixiolite structured NdNbO_4 ; (b) $(1 \times 1 \times 1)$ supercell of ixiolite structured NdNbO_4 in the direction of (a) axis.

Fig.3 The ϵ_r values and the deviations (Δ) between theoretical and observed dielectric of $\text{Nd}_{1.02}(\text{Nb}_{1-x}\text{Ta}_x)_{0.988}\text{O}_4$ ($x=0.0, 0.02, 0.04, 0.06, 0.08, 0.1$) ceramics.

Fig.4 The $Q \times f$ values and the packing fraction of $\text{Nd}_{1.02}(\text{Nb}_{1-x}\text{Ta}_x)_{0.988}\text{O}_4$ ($x=0.0, 0.02, 0.04, 0.06, 0.08, 0.1$) ceramics.

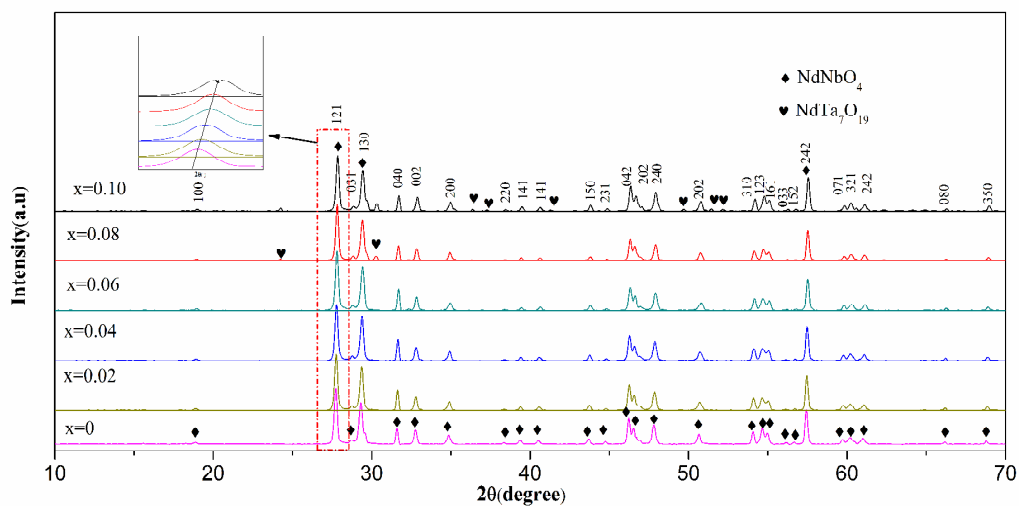


Fig.1

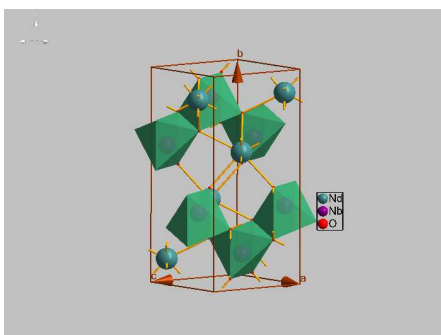


Fig.2(a)

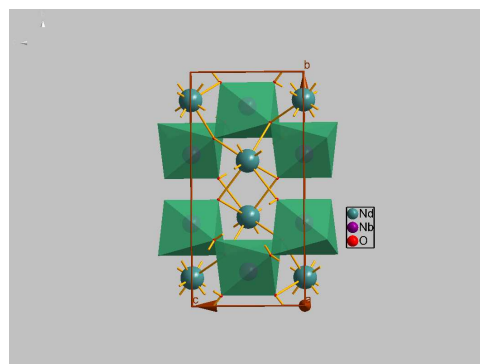


Fig2. (b)

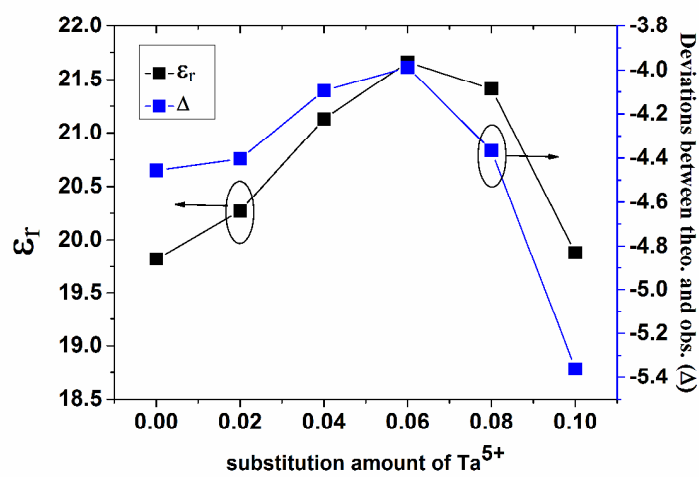


Fig.3

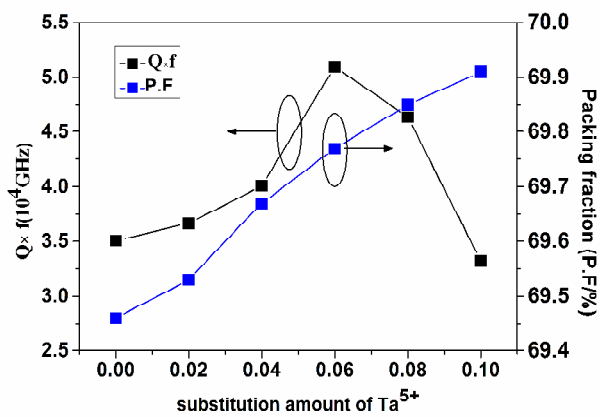


Fig. 4

A table of contents entry**Text:**

We discussed the correlation of crystal structure and microwave dielectric properties for NdNbO₄ which performs the monoclinic fergusonite structure.

